2020

A Generalized Low Order Model for Vortex Shedding From a Tandem Cylinder Arrangement Using Delay Coupled Van der Pol Oscillators

Michael Soroka
University of Central Florida

A GENERALIZED LOW ORDER MODEL FOR VORTEX SHEDDING FROM A TANDEM CYLINDER ARRANGEMENT USING DELAY COUPLED VAN DER POL OSCILLATORS

by

MICHAEL PETER SOROKA
B.S. Embry-Riddle Aeronautical University, 2011

A thesis submitted in partial fulfillment of the requirements
for the Honors in Research Program in Aerospace Engineering
in the College of the Sciences
and in the Burnett Honors College
at the University of Central Florida
Orlando, Florida

Fall Term
2020

ABSTRACT

A generalized low order model (LOM) for the fluctuating lift coefficient caused by vortex shedding from a tandem cylinder pair is proposed to expand upon models from previous authors. This model could provide a reduced computational time method for collecting qualitative and quantitive data from a tandem shedding pair. A delay coupled system with sufficient bifurcation characteristics is developed to account for the different flow regimes (extended-body, reattachment, and co-shedding) which occur as cylinder spacing is varied. Coefficient and parameter fitting is performed to fit experimental data. Finally, results and physical interpretations of the interactions in the model are discussed. It was found that many aspects of the flow at varying L/D ratios could be modeled by the LOM, including vortex suppression in the forward cylinder at the critical spacing, and amplitude growth in the rear cylinder in the co-shedding regime.

ACKNOWLEDGEMENTS

Special thanks to Professor Samik Bhattacharya, serving as my thesis chair, for guiding and mentoring me through the process of this work.

TABLE OF CONTENTS

LIST OF FIGURES

INTRODUCTION

Understanding and predicting the complex dynamics of fluid flow around bluff bodies is necessary in many engineering and design applications [1]. One topic of interest is the shedding of vortices in the near wake of structures. Vortex shedding creates periodic forces and can cause vortex-induced vibrations which often have destructive effects [7]. Intensive studies into the dynamics of different body arrangements and Reynolds Numbers have been conducted to gain insight into this phenomena.

One particular type of flow arrangement, which will be the focus of this work, is that of a tandem set of inline cylinders. This scenario is analogous to flow around pilings in a pier or adjacent buildings. Because the flow around the two cylinders is influenced by their proximity, many different and interesting dynamics occur at different spacings [1].

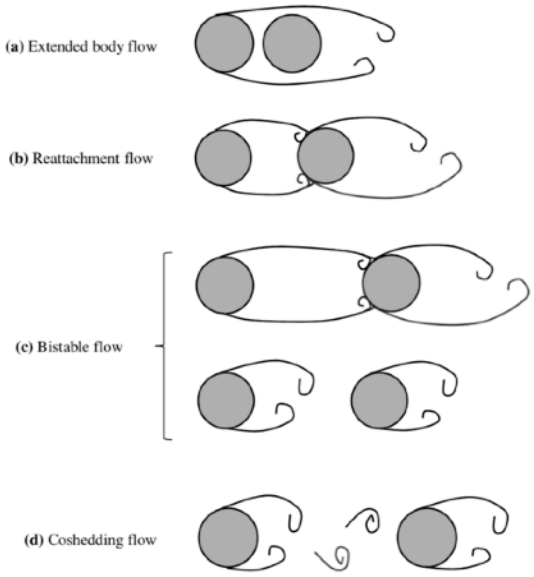

Figure 1: Schematics of possible flow structures from at different L/D ratios
[2]

Studies into this arrangement have uncovered three separate and distinct flow patterns present themselves as the Length-to-Diameter (L/D) ratio is varied: 1) “Extended-Body” regime occurring from L/D 1-2; 2) “Reattachment” regime occurring from L/D 2-5; and 3) “Co-Shedding” regime occurring at L/D > 5. These numbers are of course approximate and many aspects of the flow such as Reynolds Number have an effect on their exact value. Flow in 1) is similar to the flow around an elongated body and the pair behaves as a single entity [2]. As spacing is increased to the separation in 2), complex dynamics develop in the “gap” region between the cylinders. As the spacing is increased further, bi-stability between attached flow of the forward cylinder to the rear and periodic shedding can occur. Separation of the cylinders in 3) is sufficient for co-shedding of the cylinders to occur [2]. This co-shedding is accompanied by

frequency “lock-in” and both bodies shed at identical frequency. Of course, in extreme cases of large L/D, the cylinders behave as independent entities.

Purpose and Motivation

The computational complexity of simulations in fluid dynamics can be quite high. Low order models (LOM) are sought using simplified physics to gain insight into qualitative and quantitive aspects of the problem while greatly reducing the computational complexity. LOMs for single [3] and tandem [4] cylinder arrangements using Van Der Pol Oscillators (VDPO) to model cylinder lift coefficient (Cl) have been proposed and positive correlations between mathematical predictions and empirical data have been found. Because the dynamics of the flow varies greatly with regard to the L/D ratio in tandem cylinder arrangement, using the VDPO to model Cl has presented many challenges. As a result, models are generally proposed as in [4] at spacings where only co-shedding occurs. A coupled Van Der Pol oscillator model which could predict and model flow in all three [1), 2), and 3)] regimes would provide a more generalized and useful model, and also affirm that the usage of VDPO to model the physics of the flow in the two cylinder arrangement is just.

MOTIVATION FOR A DELAY COUPLED VDPO MODEL FOR THE TANDEM CYLINDER ARRANGEMENT

The Unforced Van Der Pol Oscillator

The basis of the LOM will rely on the Van Der Pol oscillator:

$$\ddot{x} + x - \varepsilon(1 - x^2)\dot{x} = 0 \qquad (1)$$

When the damping coefficient $\varepsilon = 0$, the equation is identical to the well-known simple harmonic oscillator (SHO). With $\varepsilon << 1$, assuming a positive value for ε, solutions are periodic and sinusoidal. Increasing ε increases the nonlinearity of the solutions, and relaxation oscillations occur. Because the Van Der Pol oscillator is a Lienard Equation, and assuming a positive damping coefficient, the conditions of the Levinson-Smith Theorem are met and the system has a unique critical point at the origin, and a unique stable limit cycle which all non-zero trajectories approach in the long run.

The usage of the unforced VDPO as a model for the fluctuating lift caused by vortex shedding from a single cylinder in fluid flow has been the subject of many publications and has been shown to provide positive qualitative and quantitive correlation to empirical data. Coefficient fitting in [3] and [8] has linked the Van Der Pol parameters to real life aspects of fluid-cylinder interaction such as lift magnitude and shedding frequency. This means using the Van Der Pol oscillator as a model for the single cylinder is justified.

The construction of a model capable of representing the complex dynamics of a tandem cylinder arrangement with variable spacing requires a system with a more varied bifurcation set. Indeed, at very large spacings, a single oscillator model could be applied to each cylinder. As the spacing between the oscillators decreases to the co-shedding regime however, mutual interactions between the cylinder wakes must be considered and frequency lock-on between the oscillators must be accounted for. It is then logical to employ some form of forcing in the proposed oscillator model to account for this.

The Forced Van Der Pol Oscillator

Again, using a single oscillator as the paradigm, the characteristics of the forced Van Der Pol oscillator in the following form are examined:

$$\ddot{x} + x - \varepsilon(1 - x^2)\dot{x} = f(t) \qquad (2)$$

This equation provides a more interesting set of dynamics. Special interest is given to cases where the forcing function is periodic. The forced Van Der Pol oscillator, where $f(t)$ takes on the form: $f(t) = bcos\omega t$, has been the subject of many studies [6]. Stability analysis with variation on parameters $b, \omega,$ and ε provides numerous disparate solution sets. Xu and Jiang [6] held ω constant at 3.1416 and analyzed the parameter plane $\mu \in [0,13]$, $b \in [0,20]$. Though they found many regions where mode-locking occurs with rational rotation numbers, they found these areas to be bordered by saddle-node bifurcation curves, and found the transition zones between them to contain more complex dynamics. This finding is critical for two reasons: 1) It provides reason to believe the destruction of the stable limit cycle in the unforced Van Der Pol oscillator is

possible, and variation of parameters could result in different solution structures and 2) It shows mode locking can occur with the forcing function. If one Van Der Pol oscillator is then forced by the solution of another, it seems logical that the dynamics of the co-shedding regime can be accounted for under certain coefficient values amenable to mode-locking.

To continue the search for the general tandem model, a system in the form (3) is examined:

$$\begin{aligned} \ddot{x}_1 + \varepsilon_1(x_1^2 - 1)\dot{x}_1 + x_1 &= 0 \\ \ddot{x}_2 + \varepsilon_2(x_2^2 - 1)\dot{x}_2 + x_2 &= F(x_1) \end{aligned} \qquad (3)$$

Where $F(x_1)$ is a delayed version of the first oscillator's solution x_1 taking the form:

$$bx_1(t - \tau)$$

Where b is the coupling parameter and τ is the time delay,

Was used by Facchinetti in [4] to model the fluctuating lift on a set of tandem cylinders in fluid flow. The solutions x_1 and x_2 were used to represent the lift fluctuations on the forward and rear cylinder respectively and parameters were fit in a similar manner used in [8]. Facchinetti used this system to model the dynamics of cylinder spacings in the "wake interference region" but beyond the spacing where proximity interference of the two cylinders occurred. This provided an excellent justification for using an unforced forward oscillator. Since the rear oscillator is coupled to the forward, wake interference from the forward cylinder can be accounted for. Further, the usage of a delay coupled forcing function on the rear oscillator allows for the time delay in the flow of the wake to be accounted for. Again, this model was shown in [4] to have

positive qualitative and quantitive similarities to the rear life interactions of the fluid flow and dynamics such as frequency lock-on and amplitude growth of the rear cylinder were observed.

Motivation for Delay Coupling

Using delay coupling in a tandem cylinder model allows for the time delay in the flow to be accounted for which greatly increases the analogy between the mathematical model and the physical world. Facchinetti showed that delay coupling can be used to model the dynamics of the tandem cylinder arrangement in the co-shedding regime. In order to generalize the model to account for the dynamics in the reattachment and extended body regimes, the dynamics of delay coupled systems are investigated further.

Wirkus [5] performed an investigation on the dynamics of two coupled Van Der Pol Oscillators with delay coupling due to the system's relevance to coupled laser oscillators. Because of the physics involved in that interaction, delay coupling via the first derivative was chosen. The system follows:

$$\ddot{x}_1 + x_1 - \varepsilon(1 - x_1^2)\dot{x} = \varepsilon\alpha\dot{x}_2(t - \tau) \qquad (4)$$

$$\ddot{x}_2 + x_2 - \varepsilon(1 - x_2^2)\dot{x} = \varepsilon\alpha\dot{x}_1(t - \tau)$$

Where α and τ represent the coupling intensity and time delay respectively. Because these types of systems become more complex to analyze, a common method employed is to decompose the system and analyze its slow flow equations. Wirkus sought equations for the slow flow for the amplitudes of the solutions and derived the following equations:

$$\dot{R}_1 = \frac{1}{2}[R_1(1 - \frac{R_1^2}{4}) + \alpha R_2 \cos(\phi + \tau)] \quad (5)$$
$$\dot{R}_2 = \frac{1}{2}[R_2(1 - \frac{R_2^2}{4}) + \alpha R_1 \cos(\phi + \tau)]$$
$$\dot{\phi} = \frac{\alpha}{2}[-\frac{R_2}{R_1}\sin(\phi + \tau) - \frac{R_1}{R_2}\sin(\phi - \tau)]$$

With the following equilibrium point:

$$R_1 = R_2 = 2\sqrt{1 + \alpha cos\tau}, \phi = 0, 1 + \alpha cos\tau > 0$$

Two results follow: 1) The amplitudes $R_i \to 0$ as $1 + \alpha cos\tau \to 0$ (amplitude death) and 2) crossing the $\alpha = -1/cos\tau$ curve in parameter space results in a bifurcation leading to a change in stability of the trivial solution of (4). These results imply variation of parameters α and τ in (4) could result in the creation or destruction of a stable limit cycle in the system accompanied by a change in stability of the fixed point at the origin.

This implies delay coupled systems of Van Der Pol oscillators could be used to model the destruction of the lift oscillations on the forward cylinder that occur as the spacing between the two cylinders is reduced.

Investigating the Dynamics of a Delay Coupled System

Analysis of system (4) by Wirkus provided excellent insight into potential dynamics of delay coupled Van Der Pol oscillators. It is important to note however that the Hopf bifurcation resulting in the change in stability of the origin of (4) resulted when solutions $x_1 \equiv x_2$. This makes (4) a poor candidate for the final model since in the extended body regime, the forward cylinder does not experience lift fluctuations while the rear cylinder does. Regardless,

understanding the mechanisms behind Wirkus's bifurcation is key to designing a delay coupled final model.

On this path, attention is given to a simpler DDE in the form:

$$\ddot{x} + \varepsilon(x^2 - 1)\dot{x} + x = b\varepsilon x(t - \tau) \qquad (6)$$

Noting two important facts:

1) Since the bifurcation in (4) requires $x_1 \equiv x_2$, the system:

$$\ddot{x}_1 + x_1 - \varepsilon(1 - x_1^2)\dot{x} = \varepsilon\alpha\dot{x}_2(t - \tau) \qquad (4)$$

$$\ddot{x}_2 + x_2 - \varepsilon(1 - x_2^2)\dot{x} = \varepsilon\alpha\dot{x}_1(t - \tau)$$

Is then logically identical to:

$$\ddot{x}_1 + x_1 - \varepsilon(1 - x_1^2)\dot{x} = \varepsilon\alpha\dot{x}_1(t - \tau) \qquad (7)$$

$$\ddot{x}_2 + x_2 - \varepsilon(1 - x_2^2)\dot{x} = \varepsilon\alpha\dot{x}_2(t - \tau)$$

And so, the equations are independent of each other and each equation should experience the bifurcation independently.

2) Although derivative coupling is used in (4), it is fundamental to the VDPO that for sufficiently small ε, the solution x(t) approaches that of the SHO and so, derivative coupling is equivalent to half-period phase shifted non-derivative coupling which can be compensated for by varying the value of τ in (6).

Combining 1) and 2) implies that (5) will also exhibit Wirkus's bifurcation.

The Destruction of the Limit Cycle

Limit cycles are isolated closed trajectories in phase space that, unlike the familiar closed orbits of the SHO, have the unique property of attracting or repelling trajectories. Limit cycles are non-linear phenomena, that is, they can only exist in non-linear differential equations and are non-conservative [9]. This means the initial energy of a system will be altered in some way as time progresses.

In the Van Der Pol oscillator (1), The mechanism behind the limit cycle's formation is the non-linear damping term:

$$\varepsilon(1 - x^2)\dot{x} \tag{8}$$

Careful inspection shows this term has the effect of "pumping up" the system when the value of x decrease below 1 in absolute value, and adding damping when x is greater than 1 in absolute value. Because (8) applies both negative and positive damping, it seems logical the system will settle into some equilibrium of the restorative and dissipative forces. This is the intuition behind limit cycle formation.

In order to take a more physical, less abstract view, (8) can be viewed as selectively adding and removing energy from the system in a manner such that a stable equilibrium is eventually achieved. Then, a reasonable mechanism for the destruction of the limit cycle in (6) is that the delay coupled forcing function is removing energy from the system at a greater rate than it can be replenished by (8), which effectively sets up a competition between the two forces. This fact motivates an energy based approach to explain the vanishing limit cycle.

Further, using energy methods allows for avoiding more complex decompositions while intuitively explaining why the limit cycle in (6) can be eliminated. Additionally, the parameter values for b and τ for which this occurs can be estimated.

The following analysis relies on the simple fact that the total energy of a system is the sum of its kinetic and potential energy.

$$E = KE + PE$$

For the Van Der Pol oscillator:

$$E = \frac{1}{2}x^2 + \frac{1}{2}\dot{x}^2$$

Taking the derivative with respect to time:

$$\frac{dE}{dt} = x\dot{x} + \dot{x}\ddot{x} = \dot{x}(x + \ddot{x})$$

From (6)

$$x + \ddot{x} = -\varepsilon(x^2 - 1)\dot{x} + b\varepsilon x(t - \tau)$$

Then, the change in energy over time is:

$$\frac{dE}{dt} = \dot{x}[\varepsilon(1 - x^2)\dot{x} + b\varepsilon x(t - \tau)]$$

Then change in energy over one period τ_v is:

$$\Delta E = \int_0^{\tau_v} \dot{x}[\varepsilon(1 - x^2)\dot{x} + b\varepsilon x(t - \tau)]$$

$$= \int_0^{\tau_v} \varepsilon(1 - x^2)\dot{x}^2 + \int_0^{\tau_v} b\varepsilon x(t - \tau)\dot{x} \qquad (9)$$

Arriving at (9) gives a representation of the change in energy over one period of the solution x(t). The first integral represents the energy of the limit cycle and the second represents the energy of the forcing function.

Assume a case where $0 < \varepsilon << 1$.

It is known when $\varepsilon = 0$, the system (6) reduces to the SHO

$\ddot{x} + x = 0$

With the solution

$x(t) = A\cos(t)$

Thus, when ε is small,

$x(t) \approx A\cos(t) + O(\varepsilon) \qquad \dot{x}(t) \approx -A\sin(t) + O(\varepsilon)$

with period $\tau_v \approx 2\pi + O(\varepsilon)$

Substituting these values into (9):

$$\Delta E \approx \int_0^{\tau_v} \varepsilon(1 - (A\cos(t) + O(\varepsilon))^2)(A\sin(t) + O(\varepsilon))^2 + \qquad (10)$$

$$\int_0^{\tau_v} b\varepsilon(\cos(t - \tau) + O(\varepsilon))(-A\sin(t) + O(\varepsilon))$$

And so, there exists three cases:

Case 1: $\Delta E > 0$ Case 2: $\Delta E = 0$ Case 3: $\Delta E < 0$

First, focus is given to the third case. In order to simplify (10), a value for A is sought where A is the amplitude of the unforced limit cycle. By setting b=0 in (10), the unforced Van Der Pol oscillator is obtained:

$$\Delta E \approx \int_0^{\tau_v} \varepsilon(1 - (A\cos(t))^2)(A\sin(t))^2$$

Since energy is constant over one period in the limit cycle, A is sought such that $\Delta E = 0$.

$$0 = \int_0^{\tau_v} (1 - (A\cos(t))^2)(A\sin(t))^2$$

$$0 = \int_0^{2\pi} (A^2\sin(t)^2 - A^4\sin(t)^2\cos(t)^2$$

$$\pi = A^2 \int_0^{2\pi} \sin(t)^2\cos(t)^2$$

$$4 = A^2$$

And so, the amplitude of the unforced limit cycle is approximately 2. Using this value as a starting point, plugging back into (9), and removing the $O(\varepsilon)$ errors, the following expression is arrived at:

$$\Delta E \approx \int_0^{2\pi} (1 - 4\cos(t)^2)4\sin(t)^2 - \int_0^{2\pi} b\,4\cos(t-\tau)\sin(t) \tag{11}$$

Since the first integral in (11) is the energy on the limit cycle, its effect can be ignored thus reducing (11) to:

$$\Delta E \approx -4b \int_0^{2\pi} \cos(t-\tau)\sin(t) \tag{12}$$

Clearly, when $\tau = \frac{\pi}{2}$, (12) would reach its most negative value. Further, if $\tau = \frac{\pi}{2}$, increasing b would further decrease (12). Based on this analysis, the following can be concluded: The values of τ and b which would cause the change in energy over one period length to be most negative are $\tau = \frac{(4n+1)\pi}{2}$, $n \in \mathrm{Z}$ and b large. The values which would cause the most positive increase in energy are $\tau = \frac{(4n+3)\pi}{2}$, and b large. The intermediate case of $\tau = \frac{4n\pi}{2}$ is not of importance for purposes of discussion.

Numerical simulation using MATLAB's dde23 algorithm were completed and the results are shown below in figures 2 through 6.

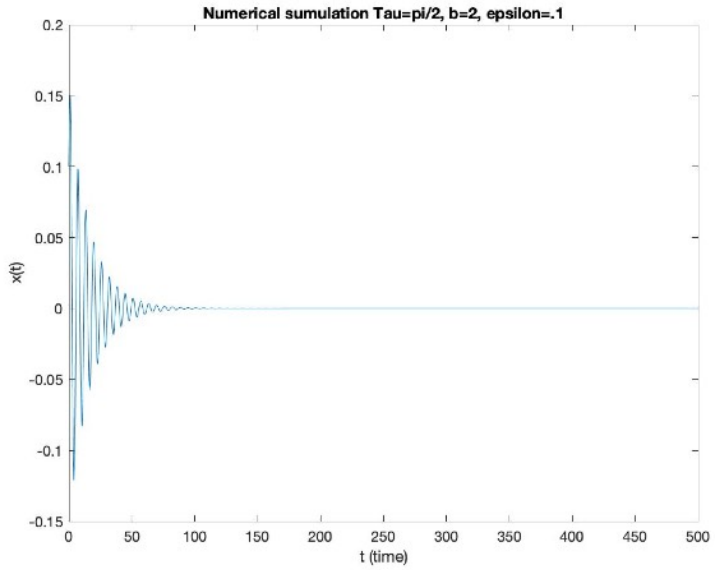

Figure 2: Numerical Simulation 1

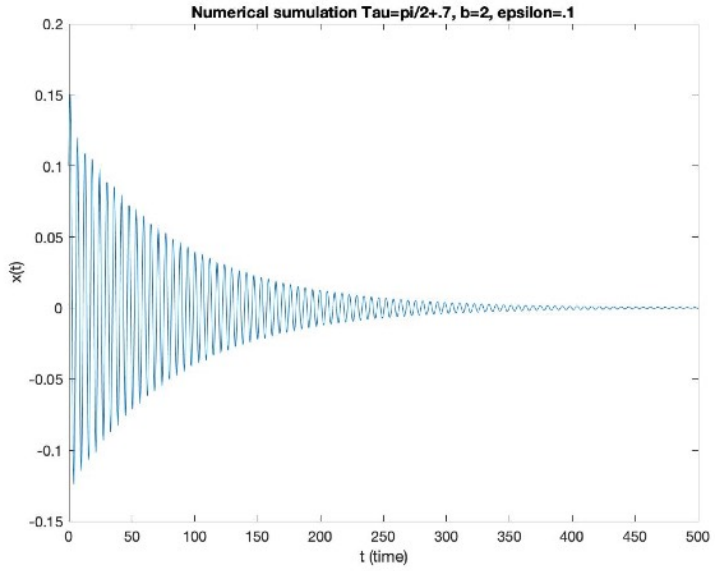

Figure 3: Numerical Simulation 2

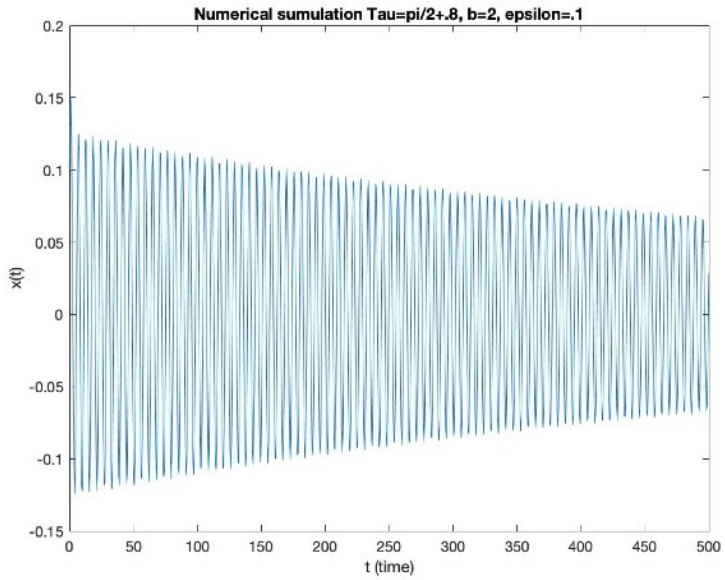

Figure 4: Numerical Simulation 3

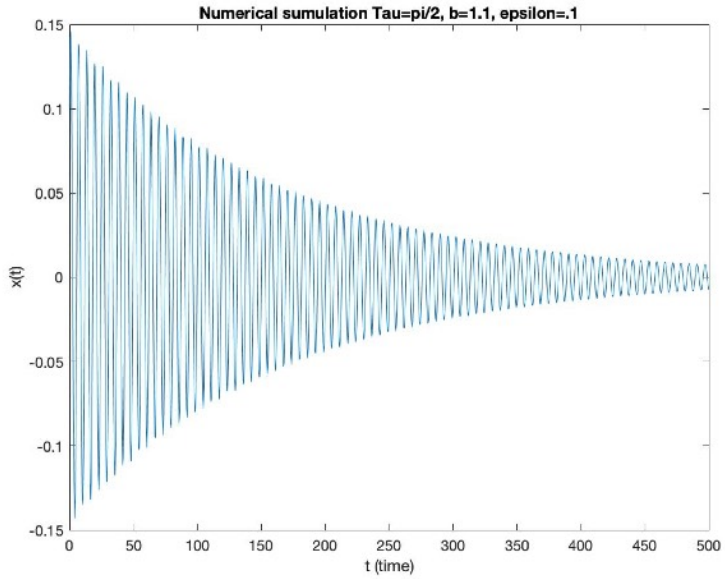

Figure 5: Numerical Simulation 4

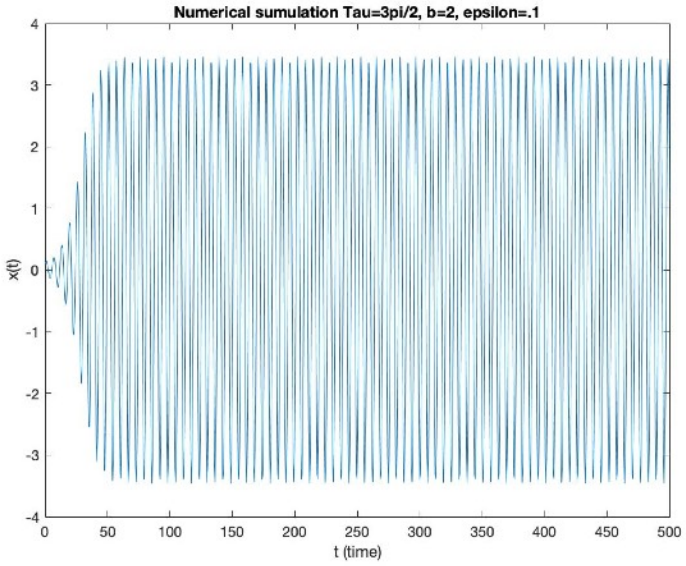

Figure 6: Numerical Simulation 5

Figure 2 shows clear destruction of the limit cycle when $\tau = \frac{\pi}{2}$ which is in agreement with the energy based assessment of (6). As suspected, a slower rate of energy dissipation is shown as τ is increased in figures 3 and 4. The theorized effect of decreasing b is also shown valid in figure 5.

So what then of case 1 where $\Delta E > 0$? Logic would dictate a monotonically increasing unbounded solution in the case where $\tau = \frac{(4n+3)\pi}{2}$, however figure 6 shows bounded periodic solutions. The answer lies again in careful inspection of (8). The restorative or "pumping" forces that add energy to system when the solution falls below 1 in absolute value can never exceed 1. Because the forcing function can defeat this effect, monotonically decreasing solutions are possible. The damping forces of (8) are unbounded however and so, increases in energy are kept in check by the fast growing x^2 term. Although the amplitude of the solution in figure 6 is higher than that of the unforced Van Der Pol oscillator, (8) is able to assure balance is achieved.

Superposition alone would predict a much higher amplitude than was observed in figure 6. In fact, the claims made in the previous paragraph allow for making anther "quick and dirty" estimation of the amplitude change in the solution based on b. Since damping grows by the square of the solution, amplitude growth in the solution would change by the root of the forcing amplitude.

Figure 7 agrees with this showing an amplitude increase over the unforced VDPO amplitude of $\sqrt{2 * 9} \approx 4$. A much more complex and accurate assessment is shown in [13].

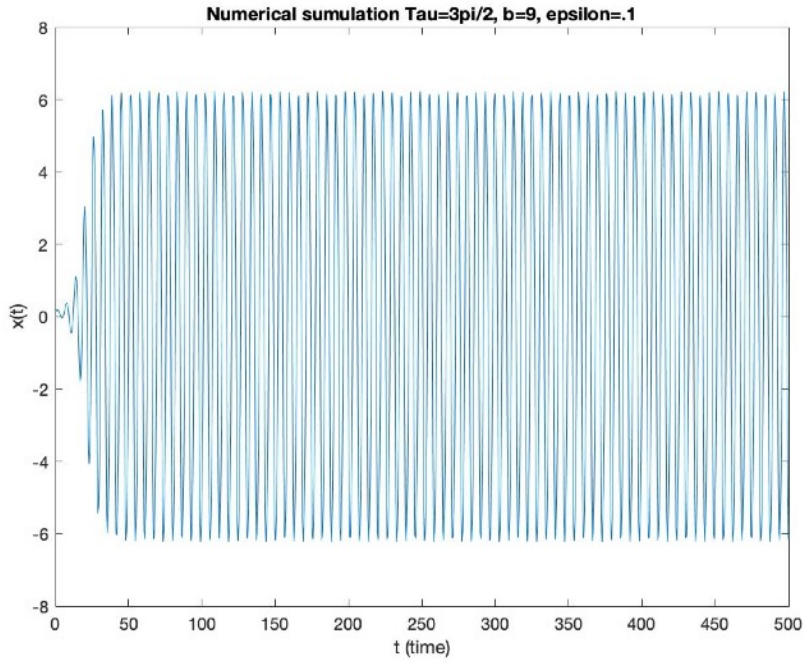

Figure 7: Numerical Simulation 6

EXAMINING A DELAY COUPLED SHEDDING MODEL

A Generalized Delay Coupled Model

Returning now to the tandem cylinder modeling problem, a system of delay coupled Van Der Pol oscillators is proposed in the form:

$$\ddot{q}_1(t) = -\mu_1 \left(\frac{\alpha_1 q_1(t)^2}{\mu_1} - 1 \right) \dot{q}_1(t) - q_1(t)\ {\omega_1}^2 + \beta_1 \mu_1 q_1\left(t - \tau_1\right) \tag{13}$$

$$\ddot{q}_2(t) = -\mu_2 \left(\frac{\alpha_2 q_2(t)^2}{\mu_2} - 1 \right) \dot{q}_2(t) - q_2(t)\ {\omega_2}^2 + \beta_2 \mu_2 q_1\left(t - \tau_2\right)$$

Where:

$q_1(t)$, $q_2(t)$ represent the lift coefficient on the forward and rear cylinder respectively

$\mu_1, \mu_2, \alpha_1, \alpha_2, \omega_2, \omega_1$ are the Van Der Pol parameters used by Nayfeh

β_1, β_2 are coupling parameters

τ_1, τ_2 are delay parameters

Using the knowledge gained in the previous chapter from investigating equation (6), it is clear that the limit cycle of q_1, representing the forward oscillator, can be broken for certain parameter values of β_1 and τ_1. Additionally, the solution's amplitude can be made to approach zero in the long run. Similarly, the amplitude of solution of the rear cylinder, q_2, can be forced to increase by the solution of the forward cylinder. These characteristics are inherent to the

proposed model and the real-life dynamical system and, along with others, will be investigated in the next sections.

Using The VDPO as a Model for Fluctuating Lift on a Shedding Cylinder

Using the Van Der Pol Oscillator to model the periodic lift fluctuations on a shedding cylinder in fluid flow is not a novel idea. The focus of this section centers on the work of Nayfeh [8], who confirmed its validity. Nayfeh first used numerical simulation to solve for the fluctuating lift on a single shedding cylinder using Reynolds-Averaged Navier Stokes (RANS) modeling. This technique provided a pressure distribution over the cylinder which was then integrated to find the resulting lift on the cylinder. Figure 8 shows the result from the RANS solution for Re= 10,000. Nayfeh found though spectral analysis that for every simulation at varying Reynolds numbers, the lift was always composed of a primary frequency, being the natural shedding frequency, and a combination of its odd harmonics.

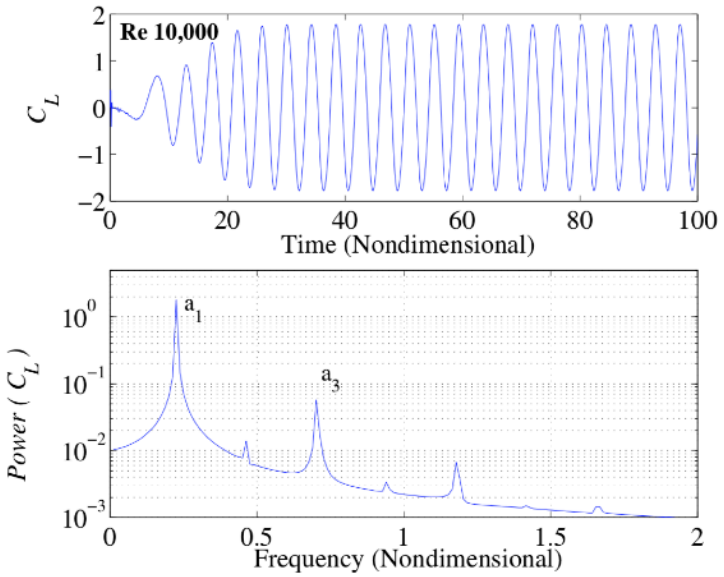

Figure 8: Result of RANS simulation from [8]

This property is also inherent to the Van Der Pol oscillator. Nayfeh proposed a Van Der Pol model in the form:

$$\ddot{q}(t) + \mu\left(\frac{\alpha q(t)^2}{\mu} - 1\right)\dot{q}(t) + q(t)\omega^2 = 0 \tag{14}$$

The results of numerical integration using MATLAB's ode45 and performing the FFT on (14) are shown in figure 9 which confirms the odd frequency components.

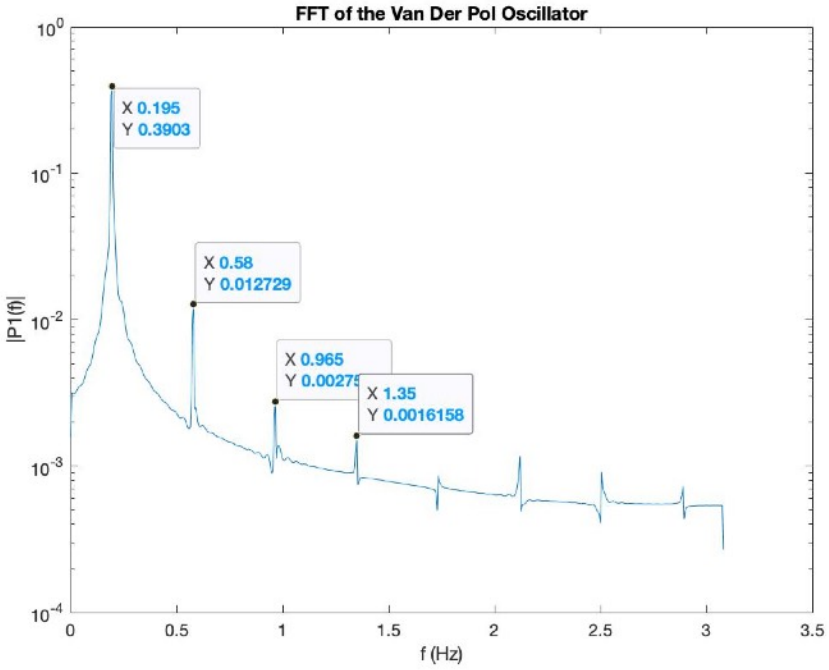

Figure 9: FFT of (9) with Mu=.06, Alpha=.66, Omega=1.21

Earlier in this work, it was mentioned the Van Der Pol oscillator, for small VDPO parameter values, has a general solution similar to that of the SHO plus an $O(\varepsilon)$ error. A much better second order approximation for the solution was found by Nayfeh using the method of multiple scales. This solution takes the form:

$$q(t) \approx a_1 \cos(\omega_s t) + a_3 \cos(3\omega_s t + \frac{\pi}{2}) + O(\varepsilon) \tag{15}$$

With

$$\omega_s = \omega - \frac{\mu^2}{16\omega} \tag{16}$$

Revealing the cause of the odd harmonic spikes in the Fourier Transform.

After performing CFD simulations, parameter values for α, ω, and μ were calculated for different Reynold's numbers completing the table in figure 10 below:

Table 1. Lift parameters at different Reynolds numbers.

	$\mathrm{Re} = 200$	$\mathrm{Re} = 10,000$	$\mathrm{Re} = 100,000$
f_s	0.19259	0.23898	0.25471
a_1	0.61470	1.79180	1.05304
a_3	0.00396	0.05816	0.02040
ω_s	1.21008	1.50156	1.60039
α	0.66030	0.48784	0.89603
μ	0.06237	0.39156	0.24840
ω	1.21028	1.50791	1.60280

Figure 10: Derived coefficients for (9) from Nayfeh [8]

(14) was then numerically integrated using these coefficients to confirm the the accuracy of the model. Both the steady state and transient lift was investigated and the results are shown below in figure 11 for Re=10,000.

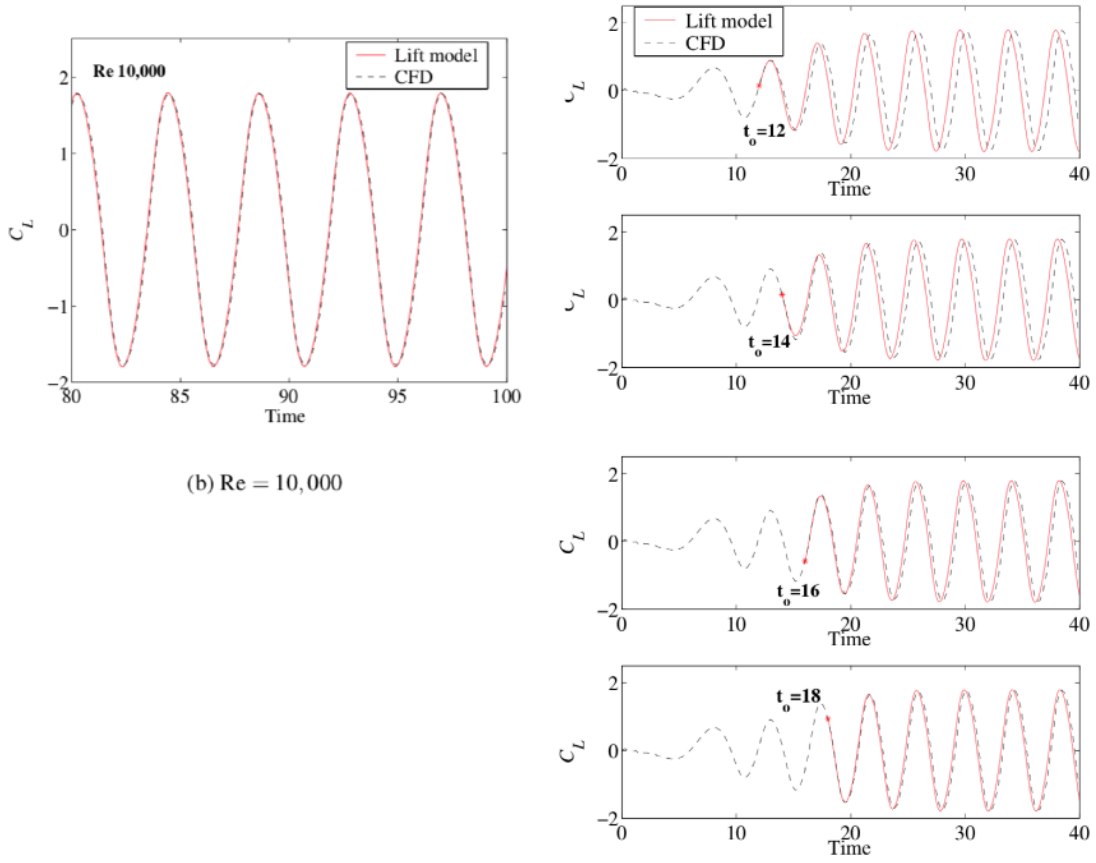

Figure 11: Steady-State and Transient Lift of CFD vs. VDPO Model From [8]

The strong correlation between the CFD and Nayfeh's VDPO model for both the steady state and transient lift confirms the Van Der Pol oscillator as an excellent model for the fluctuating lift coefficient on a shedding cylinder. Further, since correlation between the CFD and the VDPO was also found in the transient dynamics, it is likely the VDPO provides more than just simple curve-fitting, but models the physics of the interaction as well.

Forward Cylinder Suppression at the Critical Spacing

In wind tunnel experiments as well as CFD simulations, it is observed that a critical spacing exists between the cylinders where the oscillatory dynamics of the lift of the forward cylinder is suppressed. This critical spacing was found to occur at L/D spacings in the range of L/D=3.5 to L/D=4.0 for various values of Reynolds Number. It is shown in figures 12,13 that the critical spacing is relatively consistent and has only slight variation with Reynolds Number, remaining in the range of of .5 L/D for all tested flow regimes.

Source	Critical Spacing L/D	Reynolds Number	Simulation Type
Huang [10]	3.5 - 4.0	200	Particle Strength Exchange Method
Zhou [11]	3.5 - 4.0	10^3	LES
Summer [1]	3.5 - 3.8	$1 \times 10^4 - 4.5 \times 10^4$	Wind Tunnel

Figure 12: Critical spacing L/D from various sources

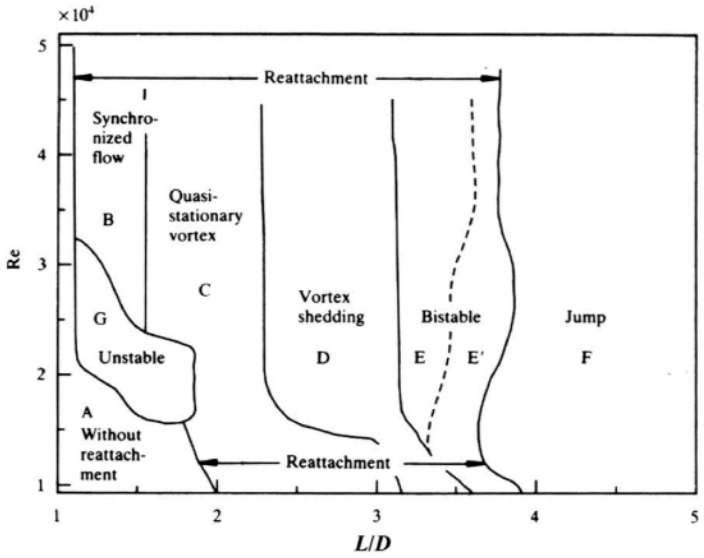

Figure 13: Flow patterns and critical spacing from Re=10,000 to Re=50,000

It was shown from the previous analysis of (6) that values of τ_1 and β_1 can be chosen such that the limit cycle normally present in the Van Der Pol oscillator will break and the amplitude of the solution will approach zero in the long run. Interest is now given to the Re=1,000 flow regime where the parameter space for τ_1 and β_1 is investigated for values where this phenomena occurs. Of course, examining a large parameter space is computationally intensive and focus is given to values such that τ_1 is its most advantageous and β_1 is minimized.

Using intuition gained from the energy-based analysis of (6), it was shown that convergence was the strongest at odd multiples of a quarter of the period length of the solution q_1. The shedding frequency was calculated using (16) and verified using MATLAB's FFT function obtaining a Strouhal Number of .200 with a period of 5. It is then logical to examine the

parameter plane around τ_1=1.25 and β_1=1. Again using MATLAB, local maximums of the solution over 1,000 time steps with $q_1(0)$=1 were found and a linear regression was performed from the 30th maximum to the final maximum to estimate the rate of decay of the solution. The results are plotted in figure 14.

		τ_1				
		1.05	1.15	1.25	1.35	1.45
β_1	0.9	p30: .4044 p120: .3941 slope: -5.442e-6	p30: .3934 p120: .3868 slope: -8.830e-6	p30: .3827 p120: .3848 slope: -1.424e-5	p30: .3914 p120: .3899 slope: -5.44e-6	p30: .4064 p120: .3939 slope: -4017e-6
	1.0	p30: .3452 p120: .3446 slope: -1.376e-5	p30: .33577 p120: .3271 slope: -2,376e-5	p30: .3264 p120: .2353 slope: -2.060e-5	p30: .3376 p120: .3259 slope: -1.853e-5	p30: .3490 p120: .3384 slope: -1.27e-5
	1.1	p30: .2921 p120: .2681 slope: -5.635e-5	p30: .2715 p120: .2456 slope: -8.079e-5	p30: .2656 p120: .2353 slope: -9.76e-5	p30: .2780 p120: .2466 slope: -8.157e-5	p30: .2867 p120: .2710 slope: -5.20e-5
	1.2	p30: .2279 p120: .1710 slope: -2.521e-4	p30: .2065 p120: .1348 slope: -3.824e-4	p30: .2038 p120: .1223 slope: -4.378e-4	p30: .2157 p120: .1409 slope: -3.641e-4	p30: .2333 p120: .1804 slope:-2.195e-4

Figure 14: Analysis of β_1xτ_1 with τ_1 near a quarter period of the solution. The 30th and 120th local maximum in the solution are plotted along with the value of the slope of the linear regression of the peaks.

Figure 14 confirms the theory that β_1 can be minimized for a value of τ_1 very near $\tau_1 = \frac{1}{4f_s}$. It is worthwhile to note the amplitude of the unforced oscillator's limit cycle for Re=1,000 is approximately .74. Additionally, the rate of amplitude reduction at τ_1=1.25 increases sharply as β_1 is increased beyond 1.2. For example, at β_1 = 1.5, p30=.0623 and p120= 3.721e-4. It is interesting to note that the dynamics of the system in this region are more rich than expected. For example, with $\beta_1 \in [.9,1.1]$, there is a large immediate drop from the unforced amplitude followed by a very slow rate of amplitude decay. When β_1 is increased to 1.4, it seems the solution never settles on this intermediate value and the amplitude begins to decay much more rapidly to zero.

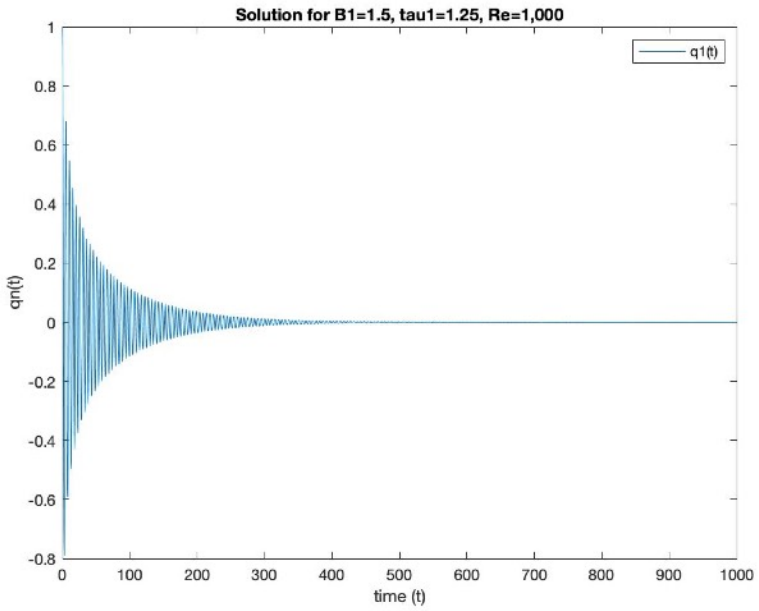

Figure 15: Solution for β_1=1.5, τ_1=1.5, Re=1,000

Wake interference in the Co-Shedding Regime

In the co-shedding regime (L/D 3.5 and greater), several notable observations are made from experimental data. First, it has been shown that the amplitude of the rear cylinder is increased due to the effect of the wake from the forward cylinder [12]. The percentage of increase in the lift coefficient is Reynolds Number dependent and is approximately 102% at Re=200 [10], 40% at Re=1,000 [11], and 50% at Re=65,000 [12]. In has also been shown that the maximum percentage increase in lift is found just before reattachment occurs, decreasing steadily as the spacing is increased [11,12]. Additionally, the shedding frequencies of the front and rear cylinder are identical [1]. Finally, and perhaps most interesting is a phase lag between the two lift oscillations is present which increases linearly with L/D [12]. Notably, reattachment occurs when the phase lag reaches 2π (figure 16).

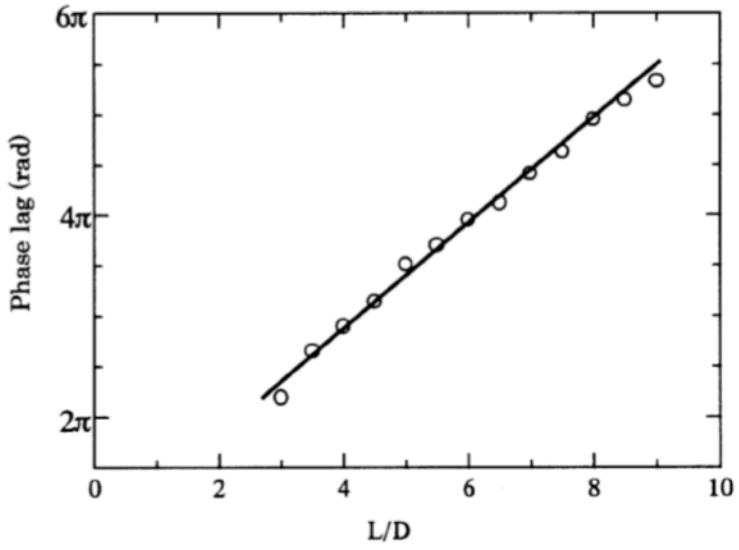

Figure 16: Variation in phase lag of fluctuating lift forces between the cylinders from [12].

The characteristics of (13) allow all of these observations to be accounted for. It is first necessary to note an important difference between the forcing of the q_1 and q_2 oscillators. In the q_1 oscillator, forcing occurs by a delayed version of its solution. This allows for the destruction of the limit cycle and the convergence observed in the previous section. This is not possible in the solution of q_2, which is forced by a delayed version of the q_1 oscillator. In this case, non-linearity allows the solution to shift and q_2 settles into a phase lag one-fourth of a period length ahead of the delay. Thus, in order to achieve a π radian phase difference between q_1 and q_2, $\tau_2 = \frac{1}{4f_s}$. Effectively, τ_2 assumes the role of shifting the phase in the solutions. The role of β_2 is to account for the amplitude growth and acts the same as in a forced VDPO. To account for the observed decrease in the amplitude of the rear oscillator as the L/D is increased beyond the critical value, β_2 must be decreased as L/D increases.

Using the experimental findings from Alam [12], conducted at Re=64,000, adjustments are made to the parameters in (13) targeting results found at L/D=4. The values of α, β, and μ were calculated as in [8]. The effect of interference from the rear cylinder on the forward is negligible at L/D=4 and so, β_1 was set to zero. A simple linear regression is used to calculate τ_2 from the data from figure 16:

$$\tau_2=\text{pi}/2 + 1.88469+ 1.67552*(\text{L/d}) \qquad (17)$$

Numerical integration was performed using MATLAB's dde23 and the results are shown below in figures 17-21.

```
mu1=.0918;
mu2=.0918;
alpha1=1.1;
alpha2=1.1;
omega1=1.2367;
omega2=1.2367;
beta1=0;
beta2=3;
tau1=2.5/2;
tau2=13.5089;
```

Figure 17: Simulation parameter values for Re=64,000, L/D=4

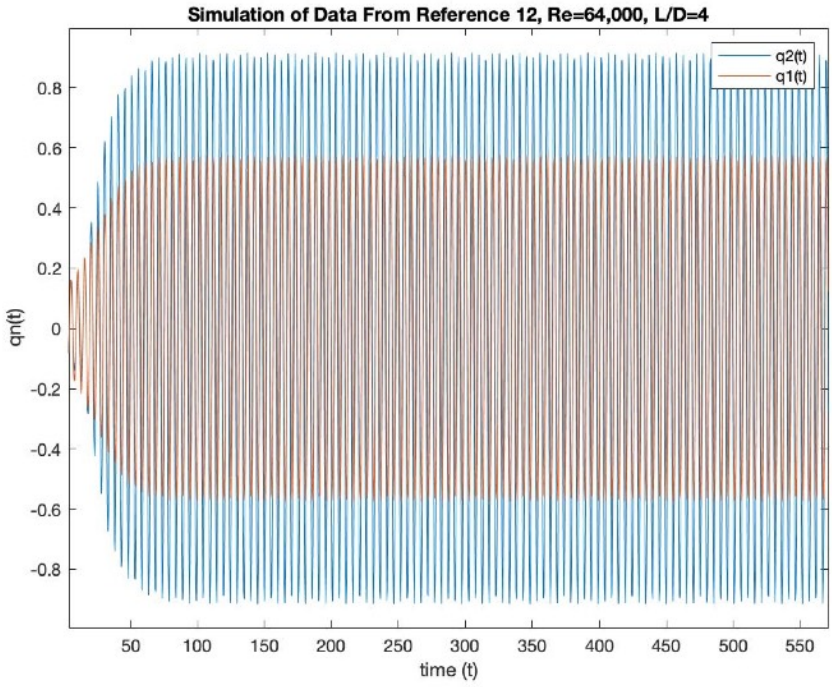

Figure 18: Numerical integration of equation 12 with solutions q1(t) and q2(t) overlaid. Initial conditions qn(0)=.1, qn'(0)=.1.

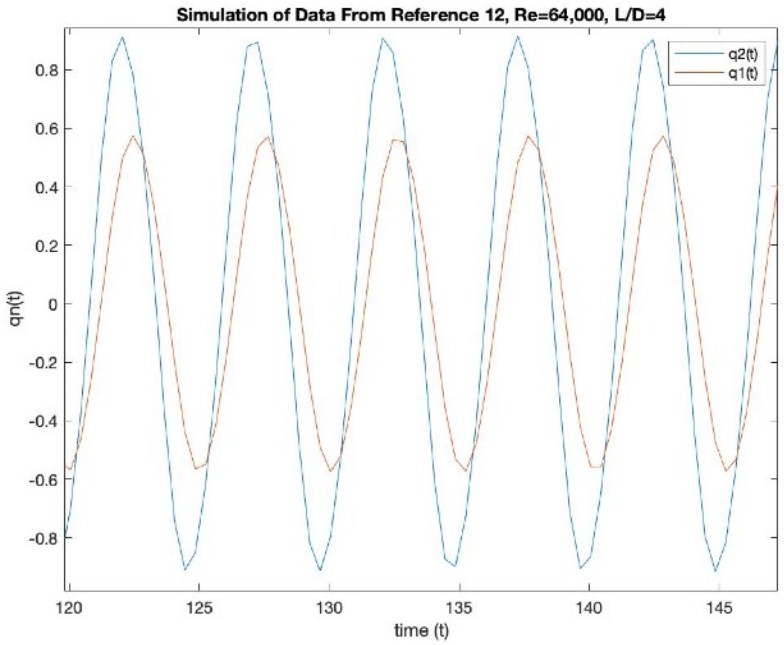

Figure 19: Zoom of figure 18 to show phase difference between q1(t) and q2(t)

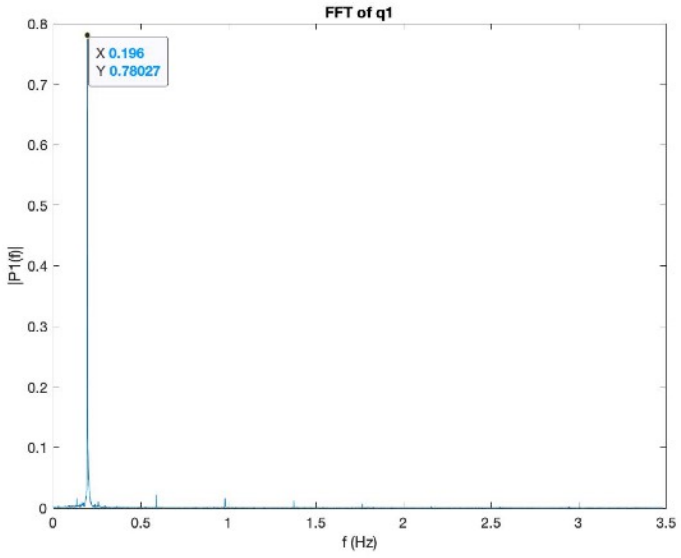

Figure 20: Fourier transform of q1(t) using MATLAB's fft function. Strouhal number is shown on the x axis.

Figure 21: Fourier transform of q2(t).

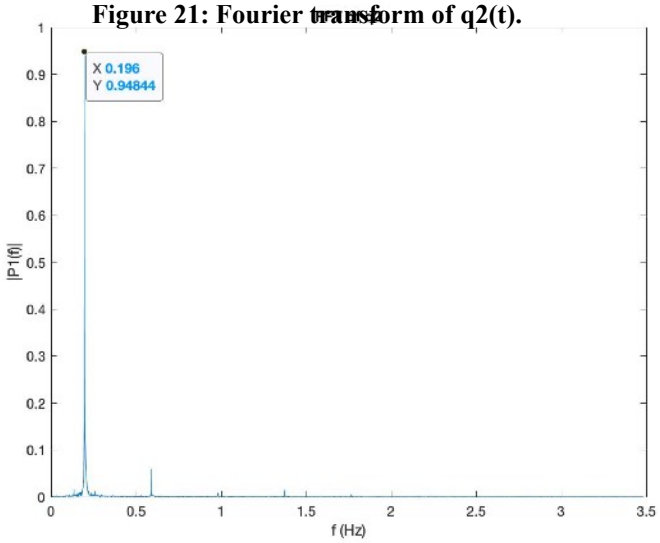

Figure 21: Fourier transform of q2(t).

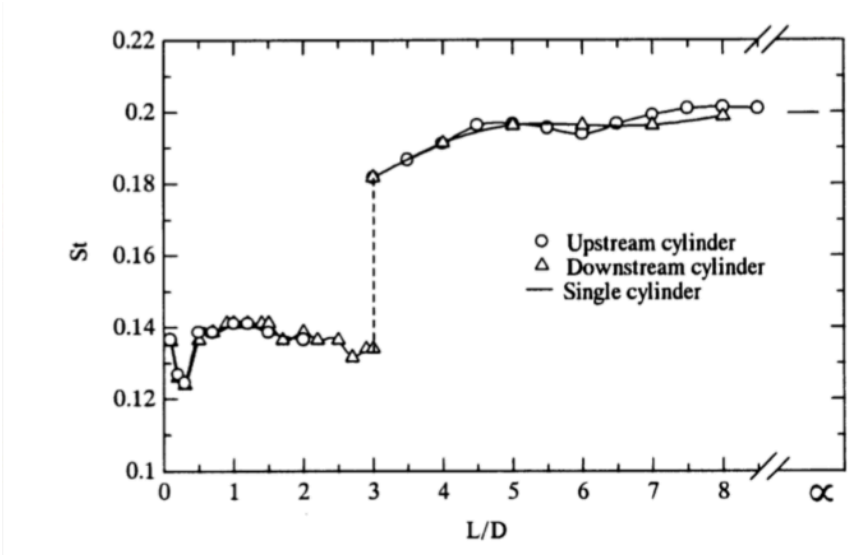

Figure 22: Strouhal number vs. L/D from empirical testing in [12]

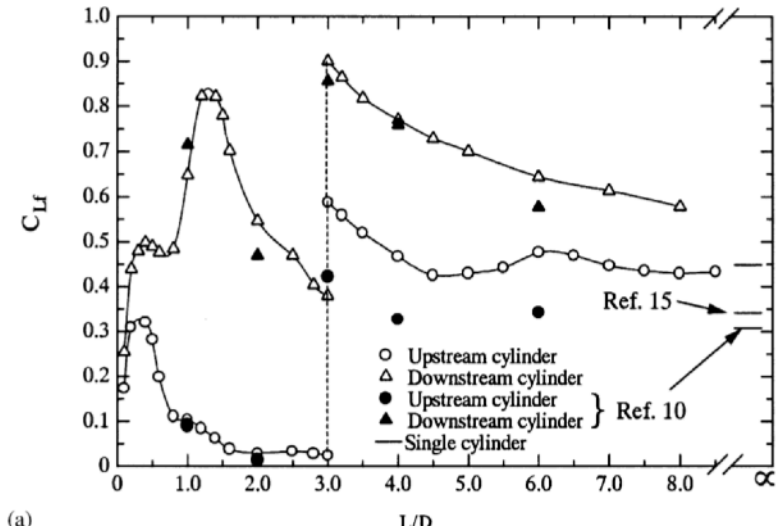

Figure 23: Coefficient of lift vs. L/D from empirical testing in [12]

A comparison of the results of figures 18-21 to the empirical data in figures 22,23 shows (13) can model many aspects of the pair at co-shedding spacings. Frequency lock-on of the q_1 and q_2 oscillators was observed with a Strouhal number of .196 in agreement with figure 22. Additionally, phase separation was achieved between the oscillators in accordance with figure 16. Finally, amplitude growth in q_2 was achieved by varying the value of β_2, allowing q_2 to be set to the value shown for the downstream cylinder in figure 23.

RESULTS, ANALYSIS, AND POSSIBLE PHYSICAL INTERPRETATIONS

In the previous chapter, several aspects of the dynamics of the tandem cylinder arrangement were shown in (13). It is now necessary to examine any physical interpretations and analyze the results of the findings.

Forward Cylinder Suppression at the Critical Spacing

It was shown that the LCO of the q_1 oscillator of (13) can be suppressed and the solution can be made to approach zero in the long run. Minimum values of β_1 and τ_1 were investigated and a non-linear rate of convergence was observed as β_1 was increased. Although β_1 could be interpreted as representing the fluid coupling or pressure feedback from the rear cylinder, such a relationship is purely theoretical. It was shown that the maximum rate of convergence was observed when τ_1 was equal to one quarter of the period length of the solution. The association of τ_1 with the length of the vortices (given Strouhal number and flow velocity) was considered however, it was shown in [10, 11, 12] that the critical spacing correlates much better to a full period length rather than a fourth. Further, since the Reynolds number was not shown to have a direct impact on the critical spacing, it is unlikely that τ_1 could be used to represent the physical aspects of the separation. It is then suggested that β_1 be made a function of the spacing and τ_1 held constant at a quarter period.

Wake Interference in the Co-Shedding Regime

The characteristics of the co-shedding regime were analyzed and a correlation between (13) and empirical data from [12] was observed. Five important characteristics seen in empirical testing are discussed:

1) Increase in rear cylinder lift: The physical explanation for the growth in lift amplitude of the rear cylinder is cited as vortex impingement from the forward [1]. Since the rear cylinder lies in the "wake interference region" of the forward cylinder, shed vortices impact the rear and an "amalgamation process" causes distortion in the shape and size of the rear cylinder's vortices.

The q_2 oscillator in (13) is delay coupled to q_1, which has an effect similar to that of the forced VDPO. β_2 controls the amount of coupling, and therefore the amplitude. In (13), the relationship of β_2 to the amplitude q_2 is non-linear and results in a much lower increase than superposition would predict. Using energy methods [13], the amplitude of the forced VDPO in the form of (2) can be estimated by the following relationship:

$$\frac{1a^3}{4} - \frac{1a^2}{2} + a = b \tag{18}$$

Where a is the amplitude of the limit cycle and b is the coupling parameter.

With the addition of the parameter α_2 in (13) however, a simple analysis such as this becomes much more complex.

2) Reynold's number dependency on lift increase: The lift increase experienced by the rear cylinder in the co-shedding regime was shown to vary at different Reynolds Numbers. Because only three flow regimes were looked at (Re=200, 1000, 64000), and with limited access to experimental data, it is difficult to comment on the mechanism behind this phenomena. The large jump in rear lift at Re=200 implies viscous forces have a large effect on the mechanism. The fact that the percentage of lift growth at Re=64,000 was higher than for Re=1,000 contradicts this however and it is likely the physical mechanism for this is more complex.

3) Lift increase maximized at critical spacing: For each Re=200, 1000, and 64000, it was shown in [10, 11, 12] that the maximum percentage of lift increase occurs immediately before the critical spacing. Additionally, in [12] it was shown this correlates to an in-phase condition of the shedding. Since an additional lift peak was observed at an L/D of two times the critical spacing, it can be deduced that the physical mechanism behind the the occurrence of the maximum at this point is due to vortex impingement.

4) Frequency lock-on: In the co-shedding regime, both cylinders shed vortices at the same frequency. In (13), the q_2 oscillator is forced by a delay coupled version of q_1. If the values of the parameters in the q_1 oscillator do not cause a large frequency variance in the solution of q_1, and if the value of β_2 is sufficient, entrainment will occur and the oscillators will exhibit frequency lock-on. It is possible that the non-linear aspects of the fluid flow are also conducive to entrainment and this is the mechanism behind frequency lock-on observed empirically.

5) Linear increase in phase lag with L/D: The linear relationship between phase lag and L/D is likely due to the shedding period in relation to the flow velocity. For example, the fact that

lift spikes were observed at multiples of the critical spacing lends to the relationship that the critical spacing is equal to the convection velocity divided by the shedding frequency. This means that τ_2 in (13) could be made a function of flow velocity and Strouhal Number.

Further Research and Conclusion

Equation (13) was shown to possess the ability to model many of the dynamics of the tandem cylinder arrangement. It is likely however that due to the complexity of interactions that can occur at different spacings, modeling every aspect of this system with simple oscillators is impossible. Further research will be needed to confirm this models efficacy in the target areas investigated.

After researching many different publications and studies on the tandem cylinder problem, a definitive reason for the mechanism of vortex suppression at the critical spacing was not found. It is then proposed an in-depth investigation be performed of the critical spacing flow, specifically looking for feedback mechanisms which could impede vortex formation in the forward cylinder. An energy argument was used to explain this phenomena in the delay coupled VDPO, where the delayed forcing function had the effect of monotonically deceasing the systems energy, acting as an energy sink. It would be interesting if a similar mechanism could be found in the real-life system.

The many aspects of the co-shedding regime translate in the dynamics of (13). Future refinements of (13) would need to directly relate β_2 to the amplitude q_2 from a mathematical perspective. Though energy methods can be used to estimate the amplitude of a forced VDPO as in (2), they become more challenging with the addition of the α_n in (13). Because this term has

the effect of controlling the energy pumping and dissipating rate, it has a dramatic and non-linear effect on the amplitude of the limit cycle. Further research into these techniques would be needed to accurately relate β_2 and q_2 amplitude.

Because such a large spike in lift increase percentage is was observed between Re=200 and Re=1,000, more data from intermediate values would be needed to make an effective assessment of the relationship between Reynolds number and lift increase in the rear cylinder. Values near Re=200 should be investigated to assure experimental findings are consistent.

Finally, the theory of entrainment of the forward and rear lift oscillations should be further investigated. Specifically whether there are there minimum values or cases, such as in (13), where frequency lock-on in the tandem pair fails to occur. Also of interest is if rear cylinder shedding is temporarily suppressed, how many cycles would it take for frequency lock-on to occur.

REFERENCES

[1] D. Sumner, "Two circular cylinders in cross-flow: A review," *Journal of Fluids and Structures,* vol. 26, pp. 850-860. Jul. 2010

[2] M. M. Alam, M. Elhimer, L. Wang, "Vortex shedding from tandem cylinders," *Exp Fluids,* vol. 59. Feb. 2018

[3] R. A. Skop, "A NonLinear Oscillator Model for Vortex Shedding From a Forced Cylinder. Part 1: Uniform Flow and Model Parameters," *In 1995 Proc. of the fifth International Offshore and Polar Engineering Conference,* pp. 578-581. Dec. 1995

[4] M. L. Facchinetti, E. de. Langre, "VIV of Two Cylinders in Tandem Arrangement: Analytical and Numerical Modeling," *In 2002 Proc. of the Twelfth International Offshore and Polar Engineering Conference,* pp. 524-531. May 2002

[5] S. Wirkus, R. Rand, "The Dynamics of Two Coupled van der Pol Oscillators with Delay Coupling," *Nonlinear Dynamics,* vol. 30, pp. 205-221. Apr. 2001

[6] J. X. Xu, J.Jiang "The Global Bifurcation Characteristics of the forced van der Pol Oscillator," *Chaos, Solitons, & Fractals,* vol. 07, pp. 3-19. 1996

[7] N. Katopodes, "Free-Surface Flow,", pp. 324-426. 2019

[8] A. Nayfeh, O. Marzouk,"Modeling the transient and steady-state flow over a stationary cylinder," *In 2005 Proc. of IDETC/CIE,* pp. 1-11. Sept. 2005

[9] C. Gang, "Fundamentals of vibrations," *Handbook of Friction-Vibration Interactions,* pp. 153-305. Jul. 2014

[10] G. Huang, H. Huan, "Simulation of Flor Past Two Tandem Cylinders Using Deterministic Vortex Method," *Thermal Science,* vol. 16, pp. 1460-1464. Jul. 2012

[11] Q. Zhou, Z.Li, "A LES Investigation of Flow Over Two Tandem Circular Cylinders at an Intermediate Reynolds Number ," *In 2017 Proc. of the 9th Asia-Pacific Conference on Wind Engineering,* Dec. 2002

[12] M. Alam, M. Moriya,"Fluctuating Fluid Forces Acting on Two Circular Cylinders in a Tandem Arrangement at a Subcritical Reynolds Number ," *Journal of Wind Engineering and Industrial Aerodynamics,* vol. 91, pp. 139-154. 2003

[13] K. Le, "Energy Methods in Dynamics,", pp. 287. Mar.29, 2015